

## Large Gate Modulation in the Current of a Room Temperature Single Molecule Transistor

Bingqian Xu,<sup>†</sup> Xiaoyin Xiao,<sup>†</sup> Xiaomei Yang,<sup>‡</sup> Ling Zang,<sup>\*,‡</sup> and Nongjian Tao<sup>\*,†</sup>

The Center for Solid State Electronics Research, Arizona State University, Tempe, Arizona 85287, and Department of Chemistry and Biochemistry, Southern Illinois University, Carbondale, Illinois 62901

Received December 18, 2004; E-mail: ntao1@mainex1.asu.edu (N.T.); lzang@chem.siu.edu (L.Z.)

The building blocks of silicon-based microelectronics are field effect transistors (FET) whose basic function is to switch electrical current between two electrodes on and off with a gate electrode. Building a single molecule FET is naturally considered to be a critical step toward the ultimate goal of molecular electronics.<sup>1</sup> While most works in molecular electronics to date have focused on two-terminal devices,<sup>2</sup> a three-terminal FET-like device is highly desired because it provides power gain, an essential requirement for large-scale integrated circuits. FET-like behavior has been demonstrated in carbon nanotubes<sup>3</sup> and nanowires,<sup>4</sup> and Coulomb blockade<sup>5</sup> and Kondo effects<sup>5b,c</sup> have been recently observed in molecular systems at low temperatures. Theoretical models have predicted that the conductance of a single molecule can be modulated with a gate electrode in the fashion of conventional FET.<sup>6</sup> Experimental demonstration of this FET behavior in single molecules has, however, been a difficult challenge because it requires one to (1) find a reliable method to wire a single molecule to the source and drain electrodes, and (2) place the gate electrode a few angstroms away from the molecule to achieve the required gate field.

Here, we demonstrate a single molecule *n*-type transistor in which the current through the molecule can be reversibly controlled with a gate electrode over nearly 3 orders of magnitude at room temperature. The molecule is wired to two gold electrodes (source and drain) via gold–thiol bonds, and the number of wired molecules is determined by statistical analysis of a large number of molecular junctions (Figure 1a).<sup>7</sup> A large gate field is achieved using an electrochemical gate in which the gate voltage is applied between the source and a gate in the electrolyte.<sup>8</sup> Since the gate voltage falls across the double layers at the electrode–electrolyte interfaces, which are only a few ions thick, a field close to  $\sim 1$  V/Å can be reached.

The molecule chosen for this work is perylene tetracarboxylic diimide (PTCDI), a redox molecule with many unique electronic properties.<sup>9</sup> It is also one of a few molecules available for use as *n*-channel materials.<sup>10</sup> To wire the molecule to two gold electrodes, we have synthesized a PTCDI derivative terminated with two thiol groups that can spontaneously bind to gold electrodes via the thiol–gold bond (Figure 1a). The energy gap between the lowest unoccupied molecular orbital (LUMO) and the highest occupied molecular orbital (HOMO) is only 2.5 eV, implying a semiconductor-like molecule. The cyclic voltammogram shows two pairs of peaks at  $-0.55$  and  $-0.8$  V (vs Ag/AgCl), respectively, corresponding to two reversible reduction processes (Figure 1b). The nominal length of the rigid molecule is about 2.3 nm, much greater than the gate thickness (the diameter of the ions), so field screening effect due to the proximity of the source and drain electrodes is

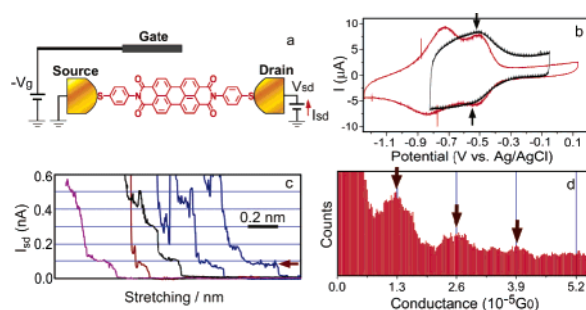


**Figure 1.** (a) Schematic of a single molecule transistor with an electrochemical gate (Ag wire reference electrode in 0.1 M NaClO<sub>4</sub>). The gate and the source-drain bias voltages are controlled with a bipotentiostat (a Pt counter electrode not shown for clarity). (b) Cyclic voltammogram of PTCDI adsorbed on gold electrode in DMF + 0.1 M TBAP (red) and in 0.01 M NaClO<sub>4</sub> aqueous solution (black). To avoid reductive desorption of the molecule, the potential was kept above  $-0.8$  V in aqueous solution. The potential sweep rate is 2 V/s. (c) Typical conductance curves during the formation of molecular junctions. (d) Conductance histogram constructed from  $\sim 1000$  individual transient curves, such as the ones shown in c.

negligible. These attributes make PTCDI an excellent candidate for resonance tunneling FET.

We wire a single PTCDI to two gold electrodes using a STM break junction.<sup>7</sup> It creates individual molecular junctions by repeatedly moving a gold tip (source electrode) in to and out of contact with a gold substrate (drain electrode), which is shown as a series of steps in the conductance (Figure 1c). Histograms constructed with 1000 individual measurements show peaks located near integer multiples of a fundamental conductance value,  $1.2 \times 10^{-5} G_0$ , where  $G_0 = 2e^2/h \approx 77 \mu\text{S}$ , with  $e$  the electron charge and  $h$  the Planck constant, which is identified as the conductance of a single molecule (Figure 1d). Such a conductance was determined at different gate voltages. The more negative the gate voltage is applied, the higher the conductance is obtained (Figure S1 in Supporting Information).

Once the conductance of a single PTCDI is determined, we pull the source and drain electrodes apart until the conductance drops to the lowest step, corresponding to a single PTCDI. We then freeze the electrodes and record the current ( $I_{sd}$ ) while sweeping  $V_g$  or  $V_{sd}$  (Figure 2). The conductance increases rapidly with decreasing  $V_g$  and reaches a peak at about  $-0.65$  V. The peak conductance is  $\sim 500$  times greater than that at  $V_g = 0$  V for a fixed  $V_{sd}$  at 0.1 V.  $I_{sd}$  can be controlled over a larger range at higher bias, due to nonlinear  $I_{sd}-V_{sd}$  curves. Figure 2b shows the  $I_{sd}-V_{sd}$  curves obtained at various  $V_g$ . At  $V_{sd} = 0.4$  V, the current can be controlled over  $\sim 1000$  times. The subthreshold slope is  $\sim 0.3$  V, close to the predictions of theoretical models for benzenedithiol molecules.<sup>6</sup>

To eliminate ionic contributions through the solution to the measured source-drain current, we coated the source electrode with Apiezon wax such that ionic conduction is  $< 1$  pA, much smaller than the lowest source-drain current measured here. The  $I_{sd}-V_g$

<sup>†</sup> Arizona State University.

<sup>‡</sup> Southern Illinois University.

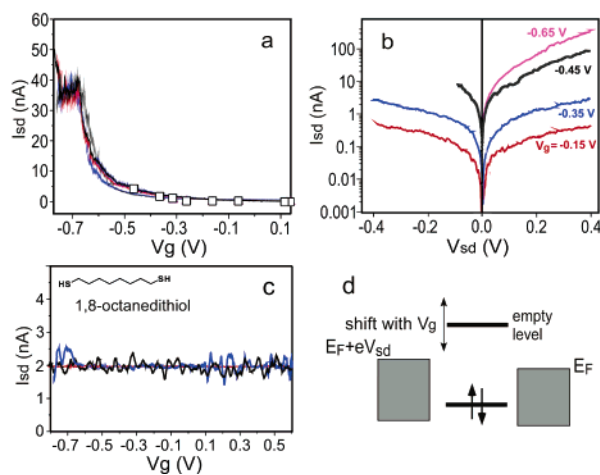


**Figure 2.** (a) Source-drain current ( $I_{sd}$ ) versus gate voltage ( $V_g$ ) for a single PTCDI molecule transistor. The open squares were obtained from the peak position of the conductance histograms (see Figure S1 in Supporting Information). The solid lines were obtained by directly recording the source-drain current while sweeping the gate voltage. (b)  $I_{sd}$  versus bias voltage ( $V_{sd}$ ) characteristic curves at various gate voltages. At low gate voltages, the curves in linear scale show the linear  $I_{sd}$ – $V_{sd}$  behavior (Figure S2 in Supporting Information). (c) Control experiment on an alkanedithiol shows no gate voltage dependence. (d) The energy diagram of the gold–PTCDI–gold junction.

curves are independent of the sweep rate, which further confirms negligible contributions from the ions. In addition, we performed the experiment by replacing the PTCDI molecule with nonredox molecules, alkanedithiols, 4,4'-bipyridine, and benzenedithiols. In all of these cases,  $I_{sd}$  is independent of the gate voltage (Figure 2c).

The large gate effect obtained with this redox molecule resembles the n-type solid-state FET (the gate sign convention here is opposite to that in solid-state electronics), but the mechanisms are different. The current peak observed here is located at  $V_g \approx -0.65$  V, close to the reduction potential of the molecule. This leads us to believe that the current enhancement is due to an empty molecular state-mediated electron transport process.<sup>11</sup> One mechanism is resonant tunneling, which predicts that the current reaches a peak when the empty state is shifted to the Fermi level by the gate (Figure 2d).<sup>6a,8a,12</sup> By considering the stochastic dynamics of solvent polarization and internal vibration modes, Kuznetsov and Schmickler<sup>13</sup> have shown that the resonant enhancement in the current through a redox molecule reaches the maximum near the redox

potential, which supports the interpretation above. An alternative mechanism that predicts a maximum current near the reduction potential is a two-step electron transport in which an electron from one electrode tunnels into the empty state to reduce the molecule and then tunnels out into the second electrode.<sup>14</sup>

**Acknowledgment.** We thank Mark Ratner, Wolfgang Schmickler, and Stuart Lindsay for valuable comments, and DOE (Xu), NSF (Xiao), and SIUC for financial support.

**Supporting Information Available:** Synthesis of PTCDI, STM break-junction measurement, Figures S1 and S2, Complete ref 5b. This material is available free of charge via the Internet at <http://pubs.acs.org>.

## References

- (1) (a) Aviram, A.; Ratner, M. *Chem. Phys. Lett.* **1974**, *29*, 277. (b) Carroll, R. I.; Gorman, C. B. *Angew. Chem., Int. Ed.* **2002**, *41*, 4379. (c) Joachim, C.; Gimzewski, J. K.; Aviram, A. *Nature* **2000**, *408*, 541.
- (2) (a) Chen, J.; Reed, M. A.; Rawlett, A. M.; Tour, J. M. *Science* **1999**, *286*, 1550. (b) Collier, C. P.; Wong, E. W.; Belohradsky, M.; Raymo, F. M.; Stoddart, J. F.; Kuekes, P. J.; Williams, R. S.; Heath, J. R. *Science* **1999**, *285*, 391. (c) Datta, S.; Tian, W. D.; Hong, S. H.; Reifenberger, R.; Henderson, J. I.; Kubiak, C. P. *Phys. Rev. Lett.* **1997**, *79*, 2530. (d) Metzger, R. M. *Chem. Rev.* **2003**, *103*, 3803.
- (3) (a) Tans, S. J.; Verschueren, A. R. M.; Dekker, C. *Nature* **1998**, *393*, 49. (b) Collins, P. C.; Arnold, M. S.; Avouris, P. *Science* **2001**, *292*, 706. (c) Javey, A.; Guo, J.; Wang, Q.; Lundstrom, M.; Dai, H. *Nature* **2003**, *424*, 654.
- (4) Cui, Y.; Lieber, C. *Science* **2001**, *291*, 851.
- (5) (a) Park, H.; Park, J.; Lim, A. K. L.; Anderson, E. H.; Alivisatos, A. P.; McEuen, P. L. *Nature* **2000**, *407*, 57. (b) McEuen, P. L. et al. *Nature* **2002**, *417*, 722. (c) Liang, W. J.; Shores, M.; Bockrath, M.; Long, J. R.; Park, H. *Nature* **2002**, *417*, 725. (d) Kubatkin, S.; Danilov, A.; Hjort, M.; Cornil, J.; Bredas, J.-L.; Stuhr-Hansen, N.; Hedegard, P.; Bjornholm, T. *Nature* **2003**, *425*, 698.
- (6) (a) Di Ventra, M.; Pantelides, S. T.; Lang, N. D. *Appl. Phys. Lett.* **2000**, *76*, 3448. (b) Damle, P.; Rakshit, T.; Paulsson, M.; Datta, S. *IEEE Trans. Nanotechnol.* **2002**, *1*, 145.
- (7) Xu, B. Q.; Tao, N. J. *Science* **2003**, *301*, 1221.
- (8) (a) Tao, N. J. *Phys. Rev. Lett.* **1996**, *76*, 4066–4069. (b) Gittins, D. I.; Bethell, D.; Schiffrin, D. J.; Nichols, R. J. *Nature* **2000**, *408*, 67. (c) Tran, E.; Rampi, M. A.; Whitesides, G. M. *Angew. Chem., Int. Ed.* **2004**, *43*, 3835. (d) Haiss, W.; Van Zalinge, H.; Higgins, S. J.; Bethell, D.; Hoebenreich, H.; Schiffrin, D. J.; Nichols, R. J. *J. Am. Chem. Soc.* **2003**, *125*, 15294.
- (9) (a) Gregg, B. A.; Cormier, R. A. *J. Am. Chem. Soc.* **2001**, *123*, 7959–7960. (b) Thelakkat, M.; Schmitz, C.; Schmidt, H.-W. *Adv. Mater.* **2002**, *14*, 577. (c) Schmidt-Mende, L.; Fechtenkotter, A.; Mullen, K.; Moons, E.; Friend, R. H.; MacKenzie, J. D. *Science* **2001**, *293*, 1119.
- (10) (a) Katz, H. E.; Lovinger, A. J.; Kloc, C.; Siegrist, T.; Li, W.; Lin, Y.-Y.; Dodabalapur, A. *Nature* **2000**, *404*, 478. (b) Newman, C. R.; Frisbie, C. D.; da Silva Filho, D. A.; Bredas, J.-L.; Ewbank, P. C.; Mann, K. R. *Chem. Mater.* **2004**, *16*, 4436.
- (11) Scudiero, L.; Barlow, D. E.; Mazur, U.; Hipps, K. W. *J. Am. Chem. Soc.* **2001**, *123*, 4073.
- (12) Schmickler, W.; Widrig, C. *J. Electroanal. Chem.* **1992**, *336*, 213.
- (13) Kuznetsov, A. N.; Schmickler, W. *Chem. Phys.* **2002**, *282*, 371.
- (14) Kuznetsov, A. M.; Ulstrup, J. *J. Phys. Chem. A* **2000**, *104*, 11531.

JA042385H